

# Analysis of heat extraction performance and long-term sustainability for multiple deep borehole heat exchanger array: a project-based study

Wanlong Cai<sup>a,b</sup>, Fenghao Wang<sup>a,\*</sup>, Shuang Chen<sup>b,c</sup>, Chaofan Chen<sup>b,c</sup>, Jun Liu<sup>a</sup>, Jiewen Deng<sup>d</sup>, Olaf Kolditz<sup>b,c</sup>, Haibing Shao<sup>b,e,\*\*</sup>

<sup>a</sup>*School of Human Settlements and Civil engineering, Xi'an Jiaotong University, Xi'an, Shaanxi 710049, China*

<sup>b</sup>*Helmholtz Centre for Environmental Research-UFZ, Permoserstraße 15, Leipzig 04318, Germany*

<sup>c</sup>*Faculty of Environmental Sciences, Dresden University of Technology, Dresden 01069, Germany*

<sup>d</sup>*Department of Building Science, Tsinghua University, Beijing 100084, China*

<sup>e</sup>*Faculty of Geosciences, Geoengineering and Mining, Freiberg University of Mining and Technology, Freiberg 09599, Germany*

---

## Abstract

In the context of reducing carbon emission, Deep Borehole Heat Exchanger (DBHE) array has a large potential in extracting geothermal energy to provide building heating in densely populated urban areas. To investigate the thermal interaction among the DBHE, a comprehensive numerical model has been built with the OpenGeoSys software, and it is validated by monitoring data from a pilot project in Xi'an, China. The long-term simulations manifest that the outlet temperature of the DBHE array has a noticeable draw-down of 4.70 °C over 20 years in comparison to the single borehole setup. The maximum difference of outlet temperature among individual DBHE can reach up to 0.88 °C over 20 years, which will lead to a shifted thermal load of 23.35 kW (12.25 % of the designed average value). Based on the predicted subsurface temperature distribution, a non-linear correlation can be established between the drawdown in working fluid temperature

---

\*Corresponding author

\*\*Corresponding author

*Email addresses:* cw1828@stu.xjtu.edu.cn (Wanlong Cai), fhwang@mail.xjtu.edu.cn (Fenghao Wang), shuang.chen@ufz.de (Shuang Chen), chaofan.chen@ufz.de (Chaofan Chen), power20113543@stu.xjtu.edu.cn (Jun Liu), dengjw16@mails.tsinghua.edu.cn (Jiewen Deng), olaf.kolditz@ufz.de (Olaf Kolditz), haibing.shao@ufz.de (Haibing Shao)

**This is the preprint of the contribution published as:**

**Cai, W., Wang, F., Chen, S., Chen, C., Liu, J., Deng, J., Kolditz, O., Shao, H.** (2021):  
Analysis of heat extraction performance and long-term sustainability for multiple deep  
borehole heat exchanger array: A project-based study  
*Appl. Energy* **289** , art. 116590

**The publisher's version is available at:**

<http://dx.doi.org/10.1016/j.apenergy.2021.116590>

and the accumulated amount of extracted heat. The finding of work implies that the thermal interaction among individual DBHE is of significance for the sustainability of the system, and comprehensive numerical modeling should be considered in the designing procedure.

*Keywords:* Deep borehole heat exchanger array, Field test, Long-term sustainability, Energy analysis, OpenGeoSys

---

## 1. Introduction

In order to achieve the goal of limiting global warming to well below 2 °C, preferably to 1.5 °C, compared to pre-industrial levels, countries all over the world are currently pursuing the transition from conventional carbon-intensive energy system to renewable and decarbonized energy supply [1]. It is worth noting that the building sector for heating, cooling, and lighting accounts for about 40% of the total energy consumption, leading to a significant environmental impact in CO<sub>2</sub> emission [2]. Within the building sector, the proportions of space heating and domestic hot water consume more than 75% [3] and 40% [4] of the energy consumption in Europe and China, respectively. For building heating, geothermal energy has attracted growing applications due to its stability, environmental friendliness and wide availability [5, 6], which possesses a considerable potential in reducing the carbon emission.

Traditionally, Ground Source Heat Pumps (GSHP) are coupled with Borehole Heat Exchangers (BHEs) to extract or inject heat out of or into the shallow subsurface to provide building heating/cooling. For commercial projects or residential neighborhoods, the high demand for thermal load often prevents its application due to the requirement on a large area to drill hundreds of BHEs, which is often not realistic in densely populated urban areas. In order to further explore the potential of geothermal energy, Rybach et al. [7] proposed the concept of Deep Borehole Heat Exchanger (DBHE) by prolonging the length of the vertical borehole to 2000 m~3000 m meter deep, and installing a coaxial pipe in it. A pilot project in Switzerland was constructed with this concept and reported by Kohl et al. [8]. By circulating fluid inside the DBHE, sensible heat stored in the surrounding rock and soil can be extracted and supplied to the building. Due to its low requirement on large land area and high thermal output, DBHE coupled heat pump has gained lots of attention throughout the world [9]. This technology is especially increasing being utilized in northern China recently, to meet the growing demand for renewable heating sources in the densely

populated urban environments. Many pilot building heating projects, extracting geothermal energy through DBHE and coupled with heat pump, have been constructed in Shaanxi, China [10].

To investigate the heat extraction performance of DBHE and its sustainability, considerable research work has been carried out in recent years. With regard to heat extraction performance, the impact of design and operation parameters has been investigated in the aforementioned studies, involving borehole depth, geological conditions, circulating flow rate etc [11]. Related work also aims at the sustainability of DBHE, especially the trend in heat extraction performance under short [12] and long-term operation period [13]. These studies are often carried out by establishing a heat transport model inside and around the DBHE, with either analytical or numerical approaches. Analytical solutions have a great advantage in calculation speed, but they may not be able to precisely handle the complex geological conditions in the deep subsurface [14, 15]. Hence numerical models were chosen by many researchers in favor of its versatility and flexibility. Numerical models are usually established with commercial and open-source modeling software, and they have already been successfully used for the analysis of heat extraction performance and sustainability of DBHE, such as using MATLAB (Finite Difference Method [16], Finite Volume Method [17]), COMSOL [18], FLUENT [19], FEFLOW [20] and OpenGeoSys [21]. In order to validate and calibrate the models, monitoring and case studies have also been carried out. Wang et al. [22] reported a commercialization project in Xi'an using DBHE coupled with heat pumps. The field test showed that a single DBHE with depth of 2000m could extract 286.4 kW of heat during the test period of ca. 5 days. Deng et al. demonstrated a series of experimental tests based on DBHE projects in Xi'an [23]. The results indicated that the heat transfer rates per length for DBHE vary from 61 W/m to 144 W/m. Bu et al. [24] and Huang et al. [25] also reported their data for model validation, which are in a short time range.

However, all the above studies are focusing on a single DBHE, which ignores the thermal interactions that may happen in a typical DBHE array. In northern China, a typical residential building project has a heated floor area from 50 000 m<sup>2</sup> to 80 000 m<sup>2</sup>, which translates to 1500 kW to 2400 kW of total thermal load. In this context, multiple DBHEs have to be linked through a pipe network, each supplying ca. 250 kW to 375 kW of thermal load [22]. On the topic of thermal interaction, plenty of work has already been reported on shallow BHE arrays, including thermal interaction examination [26], optimization method [27] and thermal performance analysis [28]. It can be clearly seen that the thermal performance of shallow BHE array

completely differs from the single BHE, due to the presence of thermal interaction. Likewise, the thermal interaction among DBHEs should not be neglected. Since the DBHEs are always used for heating only, the thermal imbalance in the subsurface is hardly avoidable. Thus, a thorough quantified analysis of the impact on thermal interaction is needed for the long-term sustainability of the DBHE array. Therefore, a series of scientific questions arise when a DBHE array is applied for building heating: Does the heat extraction performance of a DBHE array differ from a single DBHE, when the thermal interaction among DBHEs is present? If so, will this difference in heat extraction rate increase over the long-term operation, and how much thermal load will be shifted within a DBHE array?

In this work, we would like to answer the above scientific questions by both monitoring data and numerical simulation. On the monitoring side, a pilot project located in Xi'an, China was closely monitored for an entire heating season. On the numerical side, a model is first constructed based on the engineering design of the multi-DBHE array of the pilot project. The model is then validated against the monitoring data. Next, long-term simulations are carried out, and the results are compared against the single DBHE model to reveal the difference in long-term performance. Based on the simulated results, the outlet temperature drop and thermal interaction in the DBHE array are analyzed and investigated in detail. The results of this study can be instructive for long-term sustainability analysis and system design of a DBHE array heating system.

## 2. Methodology

In this section, the mathematical background, governing equations and theoretical method of the DBHE array model are introduced.

### 2.1. Model description

To investigate the proposed scientific questions, it is essential to construct and validate a numerical model that covers all features of a DBHE array. Most models mentioned in the introduction is limited to the modeling of a single DBHE. They are usually built in a two-dimensional axial-symmetric domain, and intrinsically cannot be extended to describe the thermal interactions inside a large DBHE array. On the other side, if one chooses a 3D, fully discretized numerical model, considering both the kilometer deep subsurface and millimeter-wise borehole details, the size of the mesh will explode exponentially at the location inside and near the borehole,

making it virtually impossible to manipulate the mesh with huge elements and run long-term simulations, especially for multiple DBHEs in array.

In *Heat\_Transport\_BHE* module of OpenGeoSys (OGS) [29] software, the Dual Continuum Finite Element Method (DC-FEM) [30, 31] is successfully implemented. This numerical approach was proposed by Al-Khoury et al. [32], and extended by Diersch et al [33, 34]. It has been successfully used in the analysis of borehole heat exchangers coupled heat pump system, in which the calculation speed for simulation of long-term operation is kept at an acceptable level [35]. Following the DC-FEM idea, the model domain is divided into two different compartments, which consist of the borehole and the surrounding subsurface.

For the borehole compartment, not all details are discretized and added into the finite element mesh. The boreholes themselves are treated as line elements. Hydraulic and heat processes of the borehole, including fluid circulation in the pipe, together with the associated heat transport through the grout to the soil, are simulated by governing equations on these 1D vertical line elements. For the soil compartment, 3D prism elements are used to discretize the different sediment layers. There the convective and conductive heat balance equation is solved for the 3D model domain, reflecting heat dissipation in the subsurface. This makes the number of mesh nodes in the domain to be dramatically reduced while high-level accuracy is still achieved, so that the long-term simulation of DBHE array is made possible.

The heat exchange between the borehole and the surrounding soil is then regulated by the heat flux calculation that depends on the temperature difference between the two compartments (see Fig. 1). For the BHE compartment, the heat flux leaving always means that the same amount of heat will be received by the soil compartment, and vice versa. This setup assures the overall thermal balance. For interested readers, the governing equations for heat conduction and convection deployed in the OpenGeoSys software can be found in our previous publications [36, 21].

In OpenGeoSys, the *Heat\_Transport\_BHE* process has four types of borehole heat exchangers, including 1U (single U-tube), 2U (double U-tube), CXA (coaxial pipe with annular space as the inlet downwards flow and the center part as outlet upwards flow) and CXC (coaxial pipe with a reversed flow direction). Among these types, the CXA type is proved to present a higher efficiency than others through analytical and experimental analysis [22], therefore it is chosen to be the type in our study. For the *Heat\_Transport\_BHE* process in OpenGeoSys, readers could find further information and benchmarks in the documentation on our official website [37].

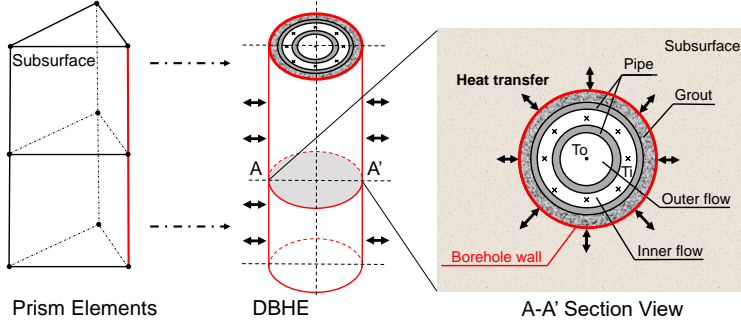


Figure 1: Heat transfer between the coaxial DBHE in borehole and surrounding subsurface

## 2.2. TESP<sub>y</sub> coupling

To depict the heat extraction performance of the DBHE array, an additional issue needed to be considered is the thermal interactions between the DBHEs. Some numerical models simply use the constant inflow temperature or impose an average value of total thermal load among all DBHEs as the boundary condition. It might not reflect the reality. In the OpenGeoSys setup, the inflow temperatures of each DBHE are treated as Dirichlet-type boundary conditions. These temperature values were calculated by the Thermal Engineering Systems in Python (TESPy) toolkit, which can simulate the coupled hydraulic-thermal process in the connecting pipe network. The setup presented in this work allows the evaluation of the actual heat extraction rate, with the subsurface thermal interaction taken into account.

To be more specific, in realistic DBHE array coupled geothermal heat pump systems, manifolds are usually installed in the system to distribute the circulating fluid to each individual DBHE, and they are also used to mix the outflow from each borehole. Thus, in order to simulate this thermal-hydraulic feature, the TESP<sub>y</sub> program has been coupled with OpenGeoSys and employed in our study. TESP<sub>y</sub> is an open-source software developed by Witte [38] that is capable of simulating the coupled thermal-hydraulic processes in thermal distribution networks. It can be used to calculate the temperature, pressure and enthalpy at each junction of the network, which is composed of predefined components such as pipe, pump, heat exchanger, etc. In TESP<sub>y</sub>, the non-linear governing equations of mass and energy balances are solved with Newton-Raphson iterations, in which the fluid properties are dynamically updated with the CoolProp library [39].

The coupling logic between OpenGeoSys and TESPpy is illustrated in Fig. 2. After calculation in OpenGeoSys at each iteration in every time step, the outlet temperature for each individual DBHE  $T_{out}$  will be sent to TESPpy through the pybind11 interface [40]. The TESPpy then will update the current status for all the components in the pipe network based on the new outlet temperature. The updated results, i.e. the new flow rate distribution and inlet temperature for each DBHE  $T_{in}$ , will be transferred back to OGS for the next iteration. If the difference between the results of the last two iterations is under the preset tolerance value, the convergence is considered to be achieved. In this study, the OpenGeoSys version 6.3.2 and the TESPpy version 0.3.2 are used accordingly. The coupling of OpenGeoSys and TESPpy has already been verified by analytical solutions (cf. [35]). More tutorials and documentation could be found on the website of TESPpy [41].

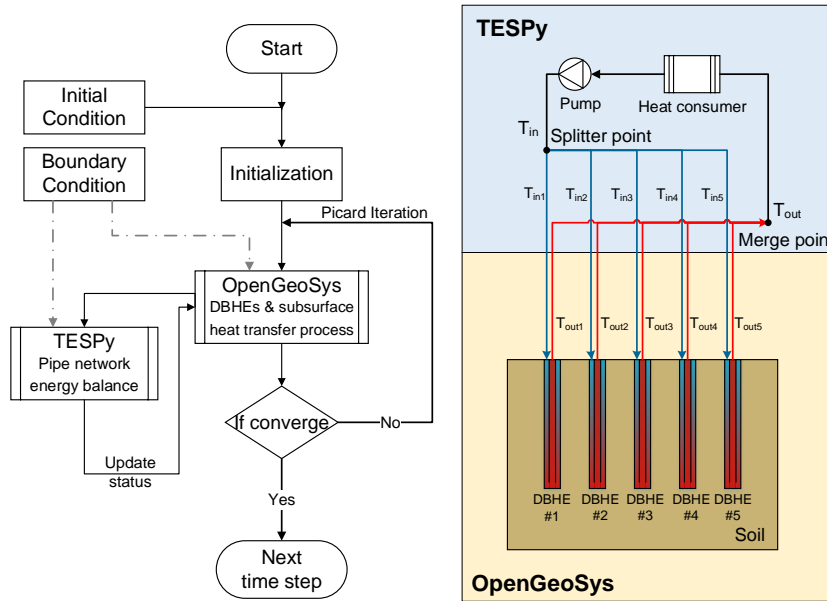


Figure 2: Schematic diagram about calculating logic between OGS and TESPpy

### 3. Pilot project and model validation

In previous published paper[42], a DBHE model established by OpenGeoSys software was validated by precise test data of a 2044 m single DBHE

for 60 days. To investigate the heat extraction performance of the DBHE array system, a pilot project located in the city of Xi'an, China has been built and closely monitored.

### *3.1. Project information and monitoring*

The pilot project with a DBHE array is built for a residential community located at  $34^{\circ}17'41.4''S$ ,  $108^{\circ}42'57.9''E$  in Xi'an city, China. The DBHE array is coupled with two heat pumps to supply heating to a neighborhood with a total floor area of ca. 56,000 m<sup>2</sup>. Five deep boreholes were drilled to a depth of 2000m and they serve as the heat source. The layout of the project is illustrated in Fig. 3. The distances among DBHE #2, #3, #4, and #5 are 15 m, while DBHE #1 and #2 are 30 m apart. All other detailed parameters of the DBHEs system are summarized in Table 1. The thermo-physical parameters of each geological stratification are measured and provided by the building construction company, and they are listed in Table 2 for reference.

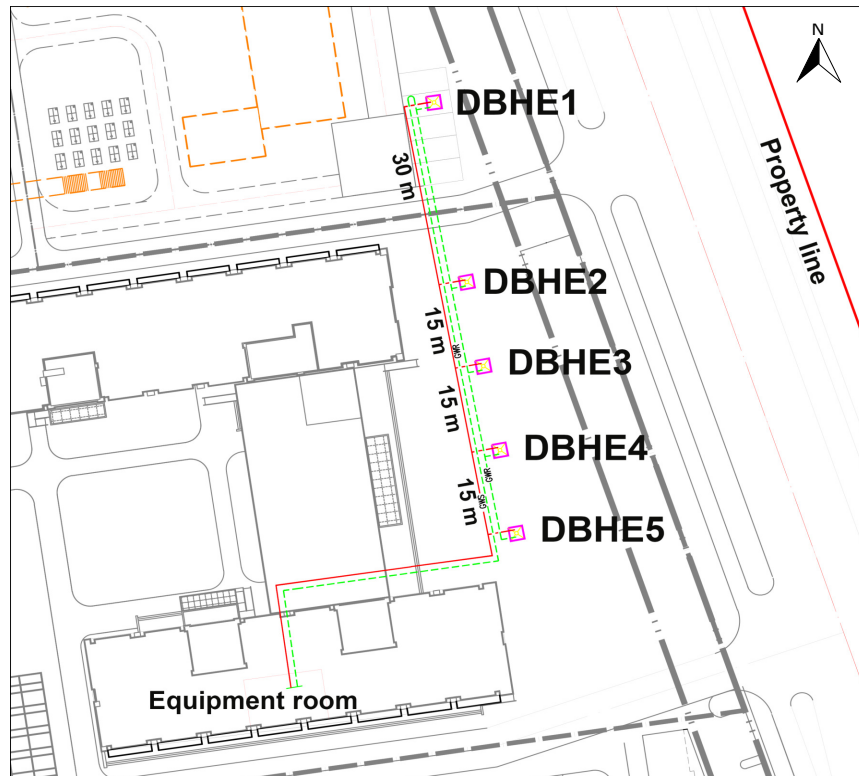


Figure 3: System layout of DBHE array in the pilot project

Table 1: Detailed parameters of the DBHE array system

Item	Parameter	Unit	Value
Borehole	Borehole depth	m	2000
	Borehole diameter	m	0.2159
	Outer diameter of inner tube	m	0.1100
	Wall thickness of inner tube	m	0.0100
	Thermal conductivity of inner tube wall	$\text{W m}^{-1} \text{K}^{-1}$	0.42
	Outer diameter of outer pipe	m	0.1778
	Wall thickness of outer pipe	m	0.0092
	Thermal conductivity of outer pipe wall	$\text{W m}^{-1} \text{K}^{-1}$	40
Circulating fluid	Density	$\text{kg m}^{-3}$	998
	Specific heat capacity	$\text{J kg}^{-1} \text{K}^{-1}$	4190
	Thermal conductivity	$\text{W m}^{-1} \text{K}^{-1}$	0.6
	Dynamic viscosity	$\text{kg m}^{-1} \text{s}^{-1}$	$9.31 \times 10^{-4}$
Grout	Density	$\text{kg m}^{-3}$	2190
	Specific heat capacity	$\text{J Kg}^{-1} \text{K}^{-1}$	1735
	Thermal conductivity	$\text{W m}^{-1} \text{K}^{-1}$	0.63
Subsurface	Geothermal gradient	$^{\circ}\text{C km}^{-1}$	33.0

Table 2: Thermo-physical parameters of four geological stratifications

Geological formation	Depth m	Thermal Con- ductivity $\text{W m}^{-1} \text{K}^{-1}$	Density $\text{Kg m}^{-3}$	Specific heat capacity $\text{J Kg}^{-1} \text{K}^{-1}$
Formation 1	0-500	1.60	1760	1433
Formation 2	500-740	1.63	1860	1025
Formation 3	740-1440	1.70	1920	978
Formation 4	1440-2200	1.81	2070	948

Since this is a pilot project, a Building Energy Management System (BEMS) was installed to monitor and record all the operational parameters related to heating, lighting and power consumption in the building. Since the monitor system was in adjustment during the starting couple of days of the heating season, monitoring data was only available starting from Nov.30, 2018 to Mar.15, 2019 (altogether 106 days in total). In this study, our purpose is to investigate the heat extraction performance of the DBHE

array. Therefore, only monitored data of inlet and outlet temperature of the DBHE array and flow rate of the ground circulation recorded at a 10 min interval was picked up from the BEMS system. This data set was also used for model calibration and validation in Section. 3.4.

### 3.2. Initial and boundary condition

For the boundary condition, since the fluctuation of air temperature at the ground surface barely has an impact on the heat extraction rate of each DBHE [21], a Dirichlet boundary condition of constant  $14.8^{\circ}\text{C}$ , which is the average ambient temperature of Xi'an, is set as the top boundary of the domain. Because the domain size is properly set to avoid that the thermal plume caused by DBHE operation will touch the side boundary. The side surfaces of domain could be set as default boundary condition which is the Neumann boundary with no heat flux. The bottom boundary is set as Neumann boundary condition with the value of  $60\text{ mW/m}^2$ , which is the normal geothermal heat flux in Xi'an. In addition, the monitored inlet temperature and flow rate are imposed on the inlet of the pipe network system as part of the boundary conditions of the numerical model. Due to the lack of monitoring data from Nov.15 to Nov.30, the average values of flow rate and inlet temperature from the nearest five days (Nov.30 to Dec.4) are set as boundary values in the numerical model for the first 15 days.

As for the initial condition, the initial subsurface temperature profile in the model follows the local undisturbed geothermal gradient with the value of  $33.0^{\circ}\text{C/km}$ , and multi-layer thermal properties are set according to the parameters listed in Table 1 and Table 2.

### 3.3. Model setup

In order to predict the long-term sustainability of the DBHE array system, a numerical model is constructed using the OpenGeoSys-TESPy model. The finite element mesh used in this model is established based on the dimension and layout of the aforementioned project design (cf. Fig. 5). In order to make sure that the thermal plume caused by DBHE operation will not interfere with the boundary of the model, the domain size is chosen to be  $200 \times 120 \times 2200\text{ m}$  (as shown in Fig. 5). The mesh is  $0.66\text{ m}$  in the vicinity of the DBHE location, and gradually becoming more sparse in the peripheral area, following the suggestions of Diersch [33]. A series of independence test were carried out involving axial and vertical grid density and also time step in Fig. 4. The results showed that, the change of element size in the axial

direction does not change the simulated outlet temperature. In the vertical direction, 50 m of mesh density is required. Larger mesh size tends to produce inaccurate temperature result. For the time step size, a maximum size of 1 h time is required to generate stable numerical results. Considering both the calculation cost and accuracy, the maximum size of axial element was assigned to 8 m while it is refined to 5 m in places close to the boreholes. (as shown in Fig. 5). The vertical mesh density was selected to be 50 m while it is refined to 10 m at the top and bottom of the domain (averagely as 27.16 m) to better quantify the geothermal gradient there. Finally, the mesh contains a total of 100,607 nodes and 194,070 elements.

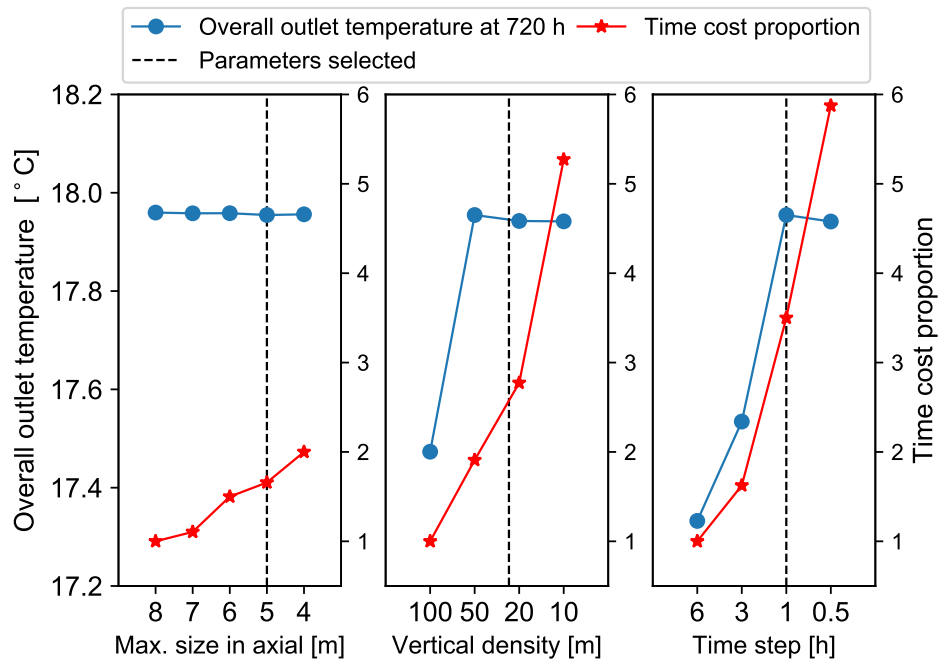


Figure 4: Predicted overall outlet temperature and simulated time under different grid density and time step

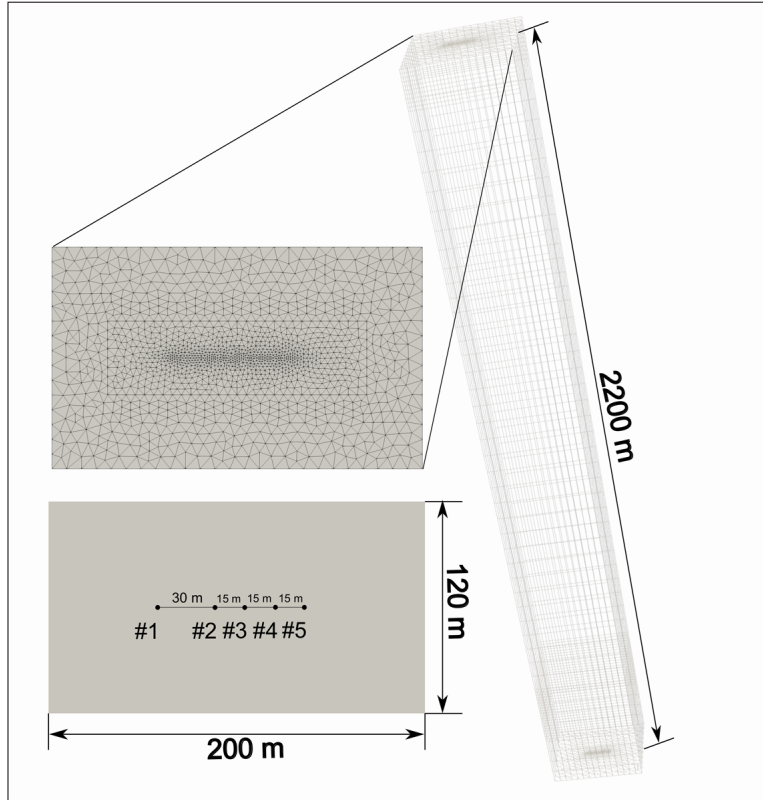


Figure 5: Overall size and mesh density of the modeling domain containing a 5-DBHE array

With respect to the pipe network, the 5 DBHEs are connected in a fully parallel manner. The same topology is constructed in the TESP<sub>y</sub> model so that the thermal-hydraulic characteristics of the pipe network could be fully captured. The temporal discretization method for our model is Backward-Euler Method. The steady-state calculation in TESP<sub>y</sub> will not be suitable to capture short-term fluctuation of the system [35] in minutes. Also, considering the time step independence test results (c.f. Fig. 4), the time step is set to be 1 h. The simulation of one heating season can be accomplished within 143 hours using a workstation equipped with a 2.20 GHz CPU and 64 GB of RAM.

### 3.4. Model validation

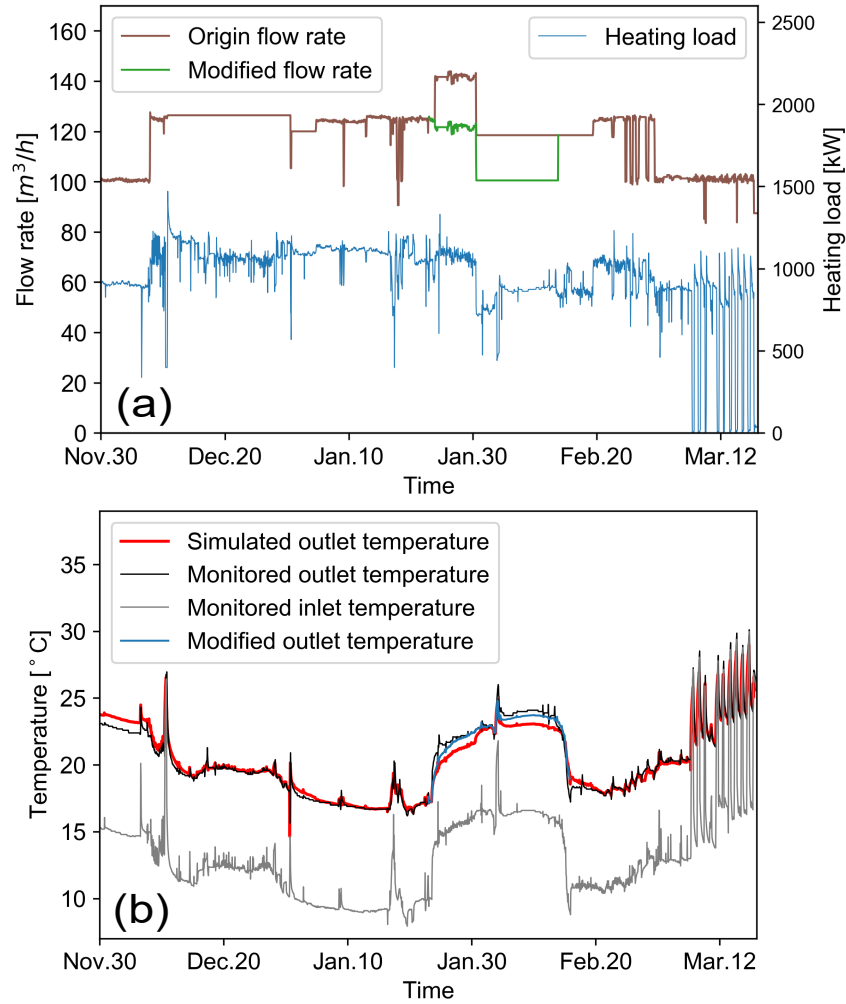


Figure 6: (a) Flow rate and overall heating load of the monitored system; (b) Validation results between monitored data and simulated results.

For the monitored heating season, the measured overall flow rate and heating load are plotted in Fig. 6(a). The monitored and simulated temperature profiles are compared in Fig. 6(b). In contrast to the monitored outlet temperature, the simulated values match the measured data quite well. At the beginning of the heating season, the difference is caused by the

average setting mentioned in Section. 3.3. In the middle part of the operation period (from Jan.25 to Feb.15), the simulated results underestimated the outlet temperature by 2.23 °C (9.54 %) in comparison to the monitored data. This sudden change of working condition is caused by a short period of trial test for another drilled borehole to assess its thermal performance. During the test, a constant flow rate was deviated away from the pipe network and used for the test. After circulation in that borehole, the water was directly discharged to the sewage system and never sent back. The short time test did not introduce thermal interference so that it was not considered in our numerical model. Accordingly, the total flow rate during the test is lowered in the model by 20 m<sup>3</sup>/h (0.0056 m<sup>3</sup>/s, the flow rate of that trial borehole), which produces a best-fitted outlet temperature curve as shown in Fig. 6(b). The relative difference between monitored and simulated values is only 1.10 °C (5.01 %), which is well below the accuracy of flow rate sensor. At the end of the heating season (from Mar.10 to Mar.15), due to the low level of heating demand, the heat pump is frequently switched on and off. This leads to a strong oscillation in the temperature profile. Yet, the numerical model is capable of capturing the oscillating feature. For the remaining majority part of the heating season, the simulated results are in good agreement with the monitored data, with the difference typically less than 0.2 °C (ca. 1%) This ensures that the coupled OGS-TESPy model has enough accuracy and is capable of capturing both the heat extraction characteristic in the subsurface and the hydraulic features in the pipe network.

Fig. 7(a) depicts the 3D cross-section view of the temperature distribution at the end of the first heating season. In terms of the outlet temperature of each DBHE, Fig. 7(b) presents the difference between the highest (DBHE #1) and lowest (DBHE #3) outlet temperature values. This suggests that the centered DBHE #3 tends to deliver a lower outlet temperature than other DBHEs, which is likely to be caused by the cold accumulation in the center of the array. Since DBHE #1 and #5 are located at the edge, the subsurface temperature recovers faster so that they have higher outlet temperatures. Especially for DBHE #1, it has the highest outlet temperature, because it is farther away from other boreholes. It is also worth mentioning that the absolute difference value for the outlet temperature is only 0.05 °C, which is hardly detectable after one heating season. However, as an increasing trend has already been observed within one season, it is unclear to us whether this difference will continue to increase over a longer operation time.

Fig. 7(c) illustrates a 2D cross-section of soil temperature distribution at the bottom of the DBHE array at the end of this heating season, and

the detailed 1D profile at 2000 m depth can be seen in Fig. 7(d). There are clear temperature drops in the vicinity of each DBHE. Moreover, the DBHE #2,#3,#4,#5 have close distance among each other so that their thermal plumes show interference with each other. Although it is only on a small scale, the thermal interference results in the different outlet temperatures of the DBHEs, as discussed above. In order to evaluate the long-term sustainability of the system, we should investigate whether the thermal interaction will enhance itself and affect the thermal performance in the long-term operation.

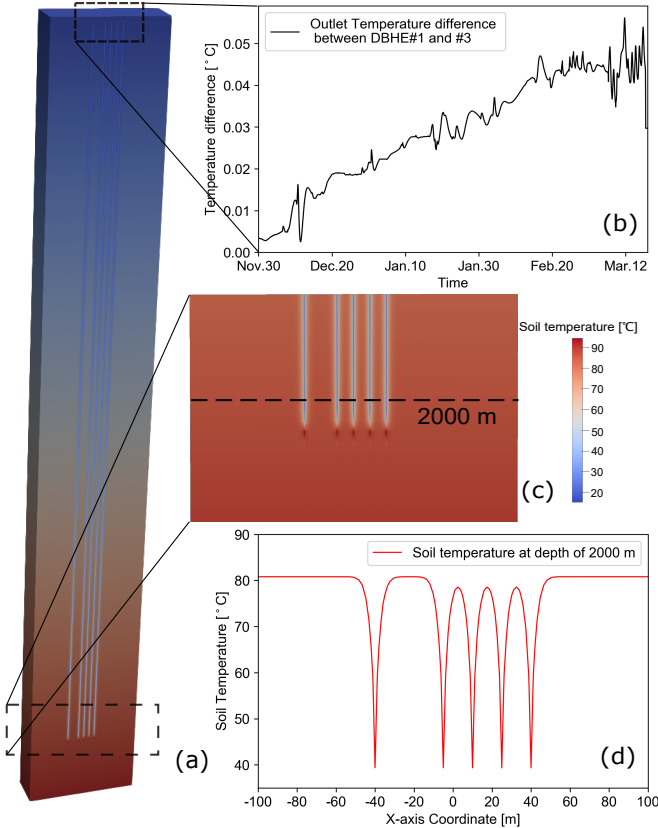


Figure 7: (a) Soil temperature field in the section view for the modeling domain; (b) Maximum temperature difference between DBHE#1 and DBHE#3; (c) Soil temperature field at bottom of subsurface; (d) Soil temperature curve after the first heating season at the depth of 2000 m

### 3.5. Extended scenario description

Since a typical HVAC system has a service life of ca. 15 to 20 years, the modeling scenario has to be simulated for the same period of time to investigate the long-term sustainability of the DBHE array. Therefore, the above-mentioned model in Section. 3 is adjusted for the long-term simulation. First, the original mesh is extended to the size of  $300 \times 200 \times 2200$  m to avoid any interference between the growing thermal plume and the horizontal no-flux boundary. And the same mesh density is also applied in the extended scenarios. Second, the hourly-wise load curve is being averaged over the entire heating season. The calculation method of total heat extraction amount for one heating season  $Q_t$  (in kWh) and average load of DBHE array  $\dot{Q}_t$  (in kW) are following Eq. (1) and Eq. (2), respectively.

$$Q_t = \int_0^{t_h} \rho_f c_f \dot{v} (T_{in} - T_{out}) dt, \quad (1)$$

$$\dot{Q}_t = \frac{Q_t}{t_h} \quad (2)$$

where  $\rho_f$  and  $c_f$  are respectively the density and specific heat capacity of the circulating fluid.  $\dot{v}$  is the volumetric flow rate of circulating fluid.  $t_h$  is the hours of heating season which is set as 2880 h.

Then, the average thermal load is imposed on the DBHE array as a power boundary condition. To be more specific, the average thermal load is set as 955.38 kW per DBHE, which corresponds to a specific heat extraction rate of 95.54 W/m. The average flow rate for DBHE array is also specified as 114.89 m<sup>3</sup>/h (0.032 m<sup>3</sup>/s). With the above treatment, the same amount of heat is extracted from the subsurface each year, and the numerical model can then be accelerated to run for 20 years.

To numerically evaluate the impact of thermal interference on the performance of DBHE array, a single DBHE is chosen to be a baseline model, as also simulated for 20 years. For this baseline model, the initial and boundary condition are kept identical to the DBHE array model, with the same initial geothermal gradient and geotechnical parameters. The same average specific heat extraction rate, i.e. 95.54 W/m, is also imposed on the single DBHE as the power boundary condition. The time step of the simulation is first set as 1 h in the heating season and increase to 6 h in the recovery season in order to reduce the calculation time. These two scenarios are all run for 20 years to investigate the differences in their heat extraction performance and long-term sustainability.

## 4. Results and interpretation

Because of the one-way heat extraction over years, the working fluid temperature will suffer an attenuation, for which the DBHE system might not sustain a stable operation. Thus, the evaluation of long-term behavior for DBHE is crucial for its sustainability. In this section, the heat extraction performance of a DBHE array is compared with a single DBHE in the long-term operation. Working fluid temperature, subsurface soil temperature distribution and heat extraction capacity between these two systems are investigated.

### 4.1. Circulation temperature

Fig. 8 compares the circulation temperatures between the DBHE array system and the single DBHE system. According to Fig. 8, it can be found that the two sets of circulation temperatures are only comparable in the first few years. With the increasing operation time, temperature from the DBHE array is consistently lower than those from the single DBHE. Also, the difference is increasingly enlarged, from  $0.14^{\circ}\text{C}$  in the first year to  $4.70^{\circ}\text{C}$  at the end of the 20th year. To maintain stable operation of the building heating system, the circulation temperature from the ground side should be no less than a critical threshold temperature, so that the freezing of circulating fluid can be avoided. Since water is usually used in the DBHE array, we set this threshold to be  $0^{\circ}\text{C}$ . In the single DBHE scenario, the minimum inlet temperature after the 20-year operation is  $6.71^{\circ}\text{C}$  at the end of the 20th heating season, which is acceptable for system operation. It is worth noting that the minimum inlet temperature for DBHE array at the 20th year is just  $2.01^{\circ}\text{C}$ , which is decreased significantly compared to the single DBHE scenario. In other words, with the same specific heat extraction rate, the single DBHE is able to maintain a higher working fluid temperature than the DBHE array. The thermal interaction among multiple boreholes in the DBHE array appears to have a negative impact on the overall outlet temperature. It can also be expected that if identical specific heat extraction rates are imposed both on the single DBHE and the DBHE array, the DBHE array system will suffer a lower heat pump efficiency, caused by the lower circulation temperature. Although the simulated temperature in the current model is higher than the  $0^{\circ}\text{C}$  threshold, it should be noticed that if a higher specific heat extraction rate were imposed, this may lead to a further deterioration of the heat pump COP and an increasing risk of system collapse.

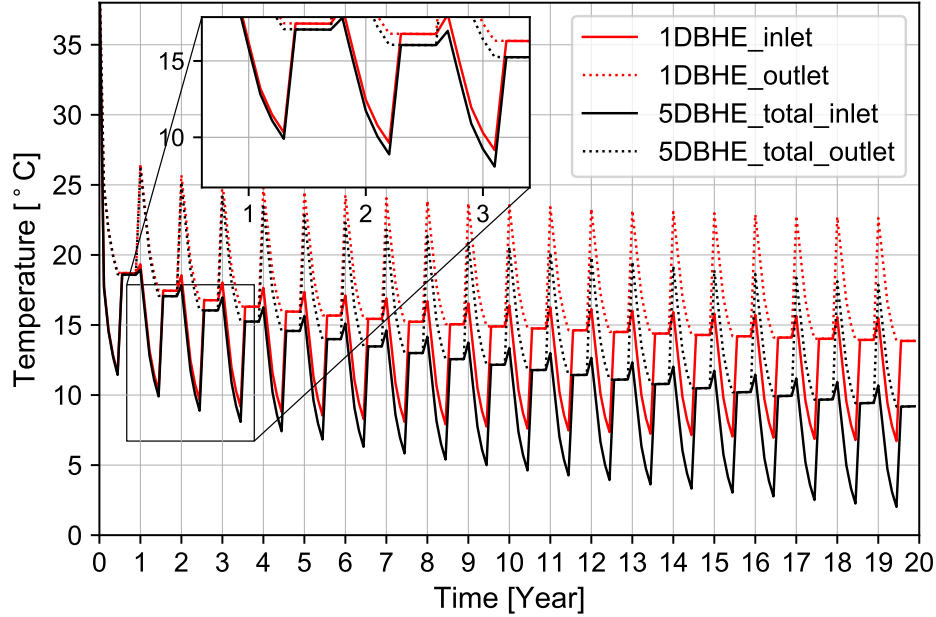


Figure 8: Overall inlet and outlet temperature for DBHE array and single DBHE for long-term operation

#### 4.2. Subsurface temperature distribution

Fig. 9 depicts the simulated subsurface temperature distribution at the 2000 m depth, with a cross-comparison between the DBHE array and single DBHE system, as well as the dynamics at the end of the heating (after the first 4 months for a year) or recovery season (at the end of a year). At the end of the heating season (Fig. 9(a) and (b)), the soil temperature profiles in both the DBHE array and single DBHE shows a sharp funnel-shaped, with the lowest soil temperature in the vicinity of the borehole location. By comparing the sub-figure (a) and (b), it is clear that the minimum soil temperature for the DBHE array is consistently lower than the single DBHE. The drop in soil temperature will be more obvious over time, which could be seen in the development of gray line (1-st year), blue line (10th year) and red line (20th year). In terms of Fig. 9(c) and (d), the Y-axis temperature range is narrowed for a better comparison. It is interesting to notice that the thermal plume keeps expanding even after the heating season, caused by the thermal conduction process driven by the lower temperature zones created during the heating season.

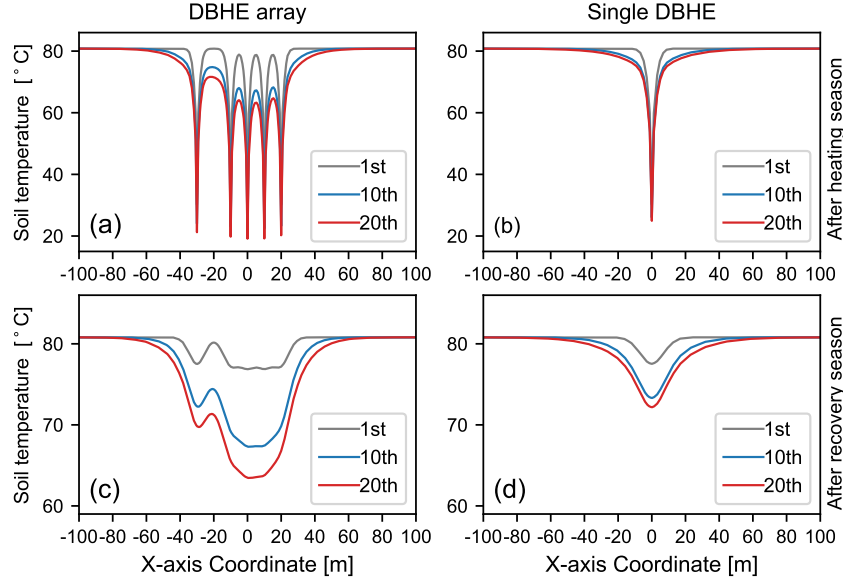


Figure 9: Soil temperature curves at 2000m depth for DBHE array and single DBHE;(a) DBHE array after every heating season;(b) Single DBHE after every heating season;(c) DBHE array after every recovery season;(d) Single DBHE after every recovery season.

Moreover, another phenomenon that can be observed in Fig. 9(c) and (d) is that the DBHE array produces a larger temperature drop and broader impact scope than the single DBHE setup after every recovery season. At the end of the first year, the difference in the soil temperature profile is not significant between the DBHE array and the single DBHE. As time goes on, the difference tends to increase. At the end of the 20-year operation, the difference is very obvious. As for the DBHE array, the funnel-shaped soil temperature curve becomes wider and deeper, which is caused by the overlap of the thermal plume of individual DBHE in the array. In terms of the soil temperature decrease, the soil temperature at the middle location (DBHE#3) is  $8.71^{\circ}\text{C}$  lower than the same location of the single DBHE. In other words, the heat interaction among individual DBHE in the array produces a stronger cold accumulation in the subsurface. Also, due to the increased distance, the soil temperature drawdown at DBHE #1 does not merge with the main drawdown area created by the other four DBHEs.

#### *4.3. Individual outlet temperature and heat extraction amount*

As for the simulated result of the DBHE array, Fig. 10(a) illustrates the outlet temperature for each individual DBHE in the array. Due to the presence of pipe network, the inlet temperatures for all DBHE are always kept at the same value. Fig. 10(b) depicts the maximum outlet temperature difference at the end of each heating season over the entire simulation period. To be more specific, the maximum outlet temperature usually occurs on DBHE #1, while the minimum can be found on DBHE #3, with the former at the edge of the array and the latter at the middle. In Fig. 10(b), the temperature difference also tends to increase over time. In the beginning, the maximum temperature difference is negligible. For instance, the maximum outlet temperature differences in the first 3 years are only 0.05 °C, 0.12 °C and 0.22 °C. Till the end of the 20th heating season, the outlet temperature for each individual DBHE can be clearly distinguished and the maximum temperature difference has reached 0.88 °C.

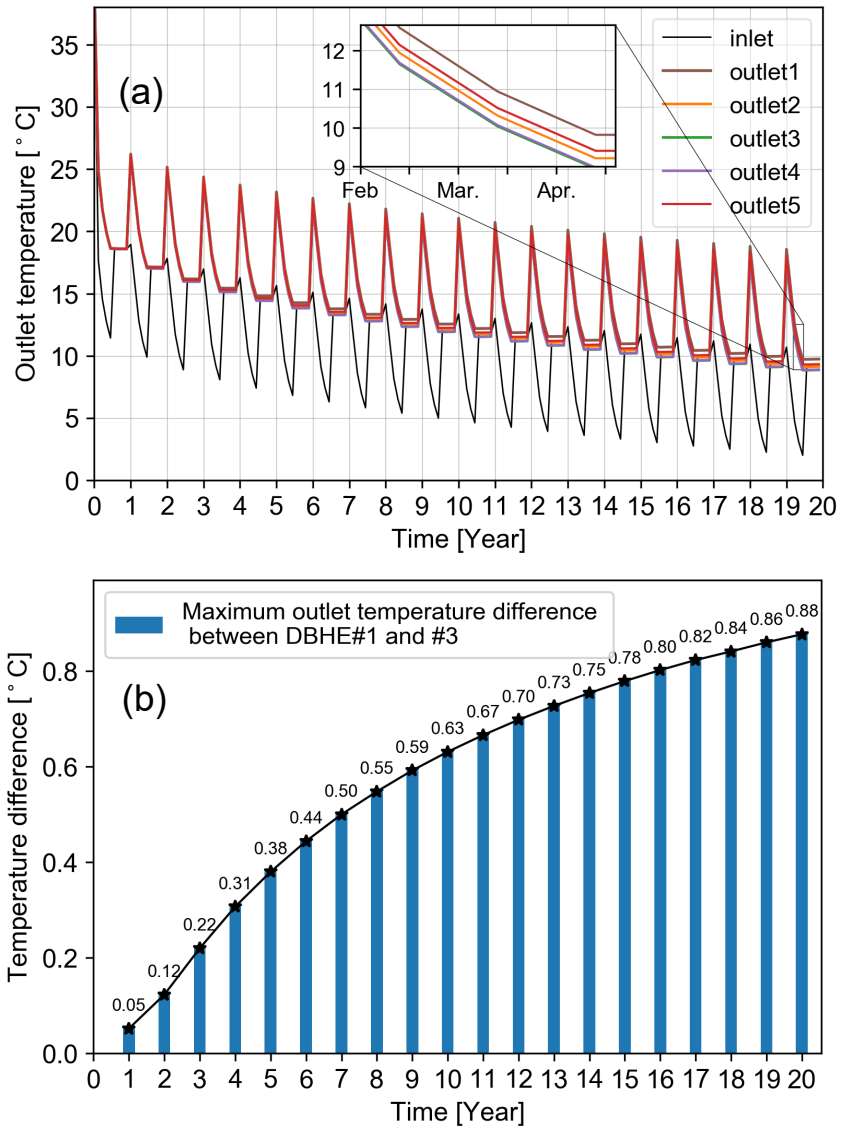


Figure 10: (a) Outlet temperature for each individual borehole in DBHE array;(b) Variation of maximum temperature difference between DBHE#1 and #3 in DBHE array.

The above phenomenon is caused by the cold accumulation in the sub-surface after long-term heat extraction. In the middle location of the array, the soil temperature reduction is more severe than at the edge (cf. Fig. 9(c)).

At the end of the first recovery season, the soil temperature in the middle of the array is only 3.94 °C lower than the initial value, which is hardly noticed. Over two decades, the cold accumulation enhances itself, leading to a severe drawdown of 17.37 °C compared to the initial value. This indicates that the drop in outlet temperature is directly controlled by the amount of soil temperature decrease, which determines the long-term sustainability of the DBHE array.

Because of the funnel-shaped soil temperature distribution, the temperature of surrounding soil for each DBHE in DBHE array differ from each other significantly. Thus, with the same inlet temperature, the actual heat extraction rate for each DBHE will not be the same. This observation is in line with the finding in our previous work (Chen et al. [35]), which showed that thermal load will gradually be shifted from the center to the periphery of the array over time in 100 m shallow BHE arrays. To show this effect, the amount of shifted load  $Q_s$  (in kW) along with its proportion  $P_s$  is quantified (following Eq. (3) and Eq. (4), respectively) and plotted for each DBHE in Fig. 11.

$$Q_s = Q_i - Q_b, \quad (3)$$

$$P_s = \frac{Q_i - Q_b}{Q_b} \times 100\% \quad (4)$$

where  $Q_i$  ( $i = 1, 2, 3, 4, 5$ ) and  $Q_b$  are respectively the actual and designed value of heat extraction rate for each DBHE in the DBHE array.

Here, the designed value of 191.08 kW for each individual DBHE is set as the baseline. The results shown in Fig. 11 suggest that the DBHE array will present the same load shifting behavior over long-term operation. In a shallow BHE array, the shifted load may even be larger than the baseline value, causing some BHEs to turn from thermal extraction to thermal recharge. Unlike the shallow BHE array, the load shifting in the simulated DBHE array is not that strong over the long-time operation. It may due to the fact that there are only five boreholes and a simple line layout for the array, which leads to relatively mild thermal interaction. In the given DBHE array, the maximum difference of heat extraction rate between DBHE #1 and #3 is 16.80 kW at the end of the 10-year operation, which is 8.8 % of the baseline value. To the end of the 20-year operation, a larger difference in heat extraction rate between DBHE #1 and #3 is estimated to be 23.35 kW, which is 12.25 % of the baseline value. It shows that, for the analysis of heat

extraction performance of DBHE array, the load shifting behavior is still existing but relatively mild.

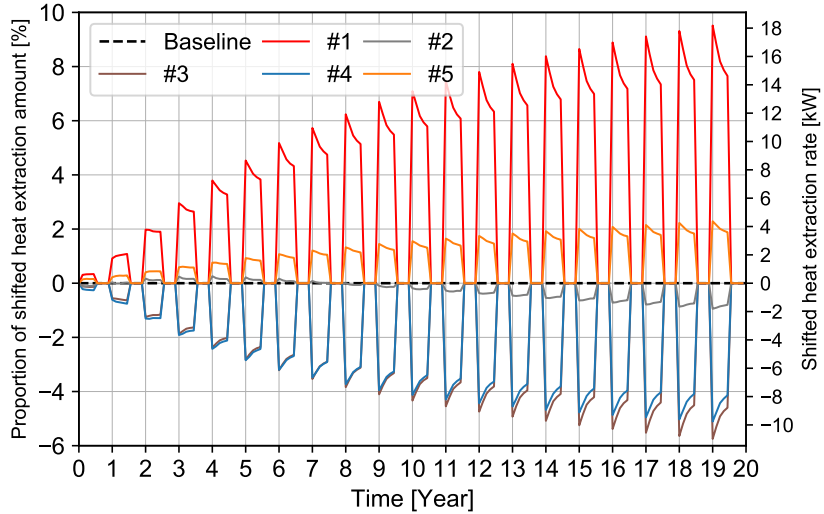


Figure 11: Load shifting behavior in DBHE array system after long-term operation

## 5. Discussion

### 5.1. Thermal plumes and design criterion

In GSHP systems coupled with shallow BHE arrays (less than 150 m deep), the thermal plumes in the subsurface often result from energy imbalance during the period of heat injection/extraction [43]. In contrast, DBHE array is only used for building heating and thus cold accumulation over the long-term is inevitable. It is hence necessary to constrain the impact of thermal plume interactions so that the negative impact on heat pump efficiency can be mitigated. In previous researches [44, 42] on DBHE, the existence of thermal plume and its impact has already been demonstrated. However, these studies do not explicitly specify the temperature threshold to define the boundary of the thermal plume. Given a preset temperature drop threshold, the boundary of the thermal plume can also vary dramatically. For example, in the single DBHE scenario simulated in this work, using 1.0 °C, 0.1 °C or even 0.01 °C of temperature threshold will yield completely distinct sizes of the thermal plumes, which range from 35 m, 60 m to 90 m,

respectively. For system designers, what needs to be estimated during the designing procedure is to identify an optimal distance among the DBHEs, so that the drop in working fluid temperature caused by the thermal plume overlapping will not severely hinder the efficiency of the heat pump. Some researchers hold the view [24] that the design criterion for a DBHE array is to adopt a proper inter-borehole distance that the thermal plume interaction is completely avoided. Following this idea, the temperature threshold of thermal plume should be as low as possible (e.g. 0.01 °C), which will result in a very large distance between the DBHEs (e.g. 90 m as shown in the simulation result).

However, DBHE arrays are mostly advantages in urban neighborhoods for building heating, where the space available for borehole drilling is very limited. Such a large inter-borehole distance proposed above is not realistic for suiting the property line of most of the DBHE projects. Actually, it is nearly impossible to completely avoid thermal plume interference in a DBHE array installed in the urban environment. A realistic target should be to identify an inter-borehole distance, that guarantees the drop of circulating fluid over the long-term is constrained in an acceptable range, and the resulting efficiency drop of heat pump is not too far away from the initial design. Following the design criterion, in which the thermal interaction is thoroughly quantified by executing comprehensive simulations and the attenuation of working fluid temperature is carefully forecast, the DBHE system will retain sustainability for long-term operation and also maintain tech-economic availability. Further research about the specific operation and workflow of this design criterion for a DBHE array system will be investigated in the future.

## 5.2. Energy perspective analysis

In a recent study [45], the temperature drop in circulating fluid was linked with the amount of accumulated energy in the subsurface. They revealed that a linear relationship can be established between these two factors, the former of which is critical for the long-term sustainability of the shallow BHE array system. In DBHE arrays, the top soil (typically 10 to 15 m deep) that is susceptible to air temperature fluctuation is negligible in comparison to the depth of the subsurface (2 km in this pilot project). As a result, the thermal recharge at the top surface can be safely neglected in numerical modeling. At the bottom of the model domain, a Neumann boundary condition is imposed in our studied model, with a constant geothermal heat flux (e.g. 60 mW/m<sup>2</sup>, cf. Hein et al. [36]). Based on results from the

aforementioned single DBHE scenario, the total amount of heat extracted from the subsurface over a heating season accounts for 550.30 MWh, which is orders of magnitudes higher than the natural geothermal recharge provided by the preset geothermal heat flux on the bottom of the domain (3.89 MWh). It manifests that the source of extracted heat comes mainly from sensible heat stored in the soil and rock surrounding the DBHEs. As discussed above, the drop in circulation temperature is critical to the long-term sustainability of the DBHE array. Thus, the relationships between temperature drop and the accumulated amount of extracted heat are plotted in Fig. 12. There, the average inlet temperature at the end of the first heating season is used as a baseline, and the trends in both the average inlet temperature  $\Delta T_{in,average}$  and annual minimum inlet temperature  $\Delta T_{in,min}$  are revealed. It could be found that the working fluid temperature reduction over long-term operation follows an exponential curve with the accumulated amount of extracted heat. The temperature drop is fast in the starting couple of years and approaches a fixed value over the long-term.

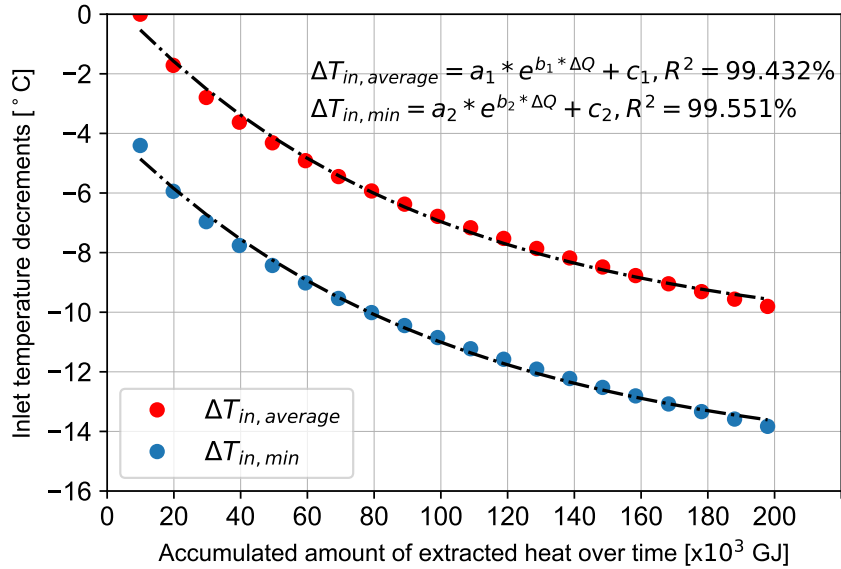


Figure 12: Non-linear correlation between the working fluid temperature decrements and the accumulated amount of extracted heat during the long-term simulation of DBHE array

Furthermore, the parameters in this exponential correlation can be well fitted. R-squared values of 99.432% and 99.551% can be achieved with the

coefficients  $a_1 = 11.617$ ,  $b_1 = -1.061 \times 10^{-5}$ ,  $c_1 = -10.983$  and  $a_2 = 11.384$ ,  $b_2 = -1.010 \times 10^{-5}$ ,  $c_2 = -15.154$ , respectively. It could be seen that the fitted curve is flattening over time, because with the increase of time, the size of thermal plume also extends, leading to an enhanced thermal recharge from the surrounding soil. Eventually, the amount of thermal recharge will reach an equilibrium with the temperature drop, which the latter will be stabilized at a fixed value. Although this is just a preliminary result, the influential factors for this interesting correlation, involving geotechnical parameters and system layout, are quite worthy to investigate in the future. This proposes another perspective that it could be possible to forecast the long-term sustainability for DBHE array by annual heat extraction amount.

### 5.3. Future work

As pointed out in the introduction part, the DBHE-based building heating system was first proposed and reported by Prof. Rybach and Prof. Kohl in Europe. There have been several pilot projects in Germany, Switzerland, and the US. In recent years, this technology is getting popular in China due to the high demand for building heating in the newly developed urban area and the low drilling cost there. Although the monitoring data presented in this work is located in Xi'an, China, the underlying physical processes and the validated numerical modeling tools, are universal and can be applied in many places of the world.

As for the future work in the field of DBHE array heating technology, further analysis of the potentially influential factors on the heat extraction performance, including the geotechnical parameters of the subsurface and load characteristics of the building side, should be investigated in order to accurately assess the heat extraction capacity of the DBHEs array heating system in different regions. Furthermore, the discussed scenarios in this study are based on a pilot DBHE heating project, for which the layout and ground load are all strictly set up according to the real project. The optimization of borehole distance and pipe network layout is also worthy of investigating, so that specific guidance can be given regarding how to properly choose these parameters in design.

## 6. Conclusion

In this study, a comprehensive numerical model is constructed to simulate the long-term behavior of a DBHE array installed in Xi'an, China. Monitoring data from the pilot project was recorded over one entire heating

season and used for model validation. The modeling results are evaluated to reveal the long-term heat extraction performance and system sustainability of the DBHE array, and they are compared to the single DBHE. To be more specific:

- The thermal interaction in DBHE array at the end of the first year is minor. After one heating season, the maximum outlet temperature difference among individual DBHEs in the array is about 0.05 °C. The thermal interaction among different DBHEs can hardly be observed. In one-year short period operation, the thermal interactions among individual DBHE in the array can be neglected.
- After 20 years, the differences in outlet and soil temperature are considerably different between the single DBHE and array setup. Based on the simulation results, the difference in overall outlet temperature is up to 4.70 °C, and the maximum soil temperature difference is 8.71 °C at the end of the 20-year period. In a regular arrangement with a 15 m distance, the DBHE array suffers more attenuation in heat extraction performance than the single DBHE in the long-term. Therefore, the thermal interactions in DBHE array cannot be ignored in the long-term, and it should be carefully considered when designing the system.
- The heat extraction performance of individual DBHE differs from each other at different locations of the array. The maximum temperature difference of individual DBHE can reach 0.88 °C, which is observed on boreholes located in the middle and at the edge of the array. This deviated outlet temperature yield a shifted thermal load of 23.35 kW, which accounts for 12.25 % of the average design value. As a result, long-term thermal interaction induced load shifting behaviors in the DBHE array are not severe but can not be ignored.
- A non-linear correlation can be well established between the working fluid temperature decrements and the accumulated amount of the extracted heat. This correlation can be applied to forecast the long-term sustainability of DBHE array.

In the current designing procedure of DBHE array, most engineers assume that there exist no thermal interactions among the multiple DBHEs. With this assumption, it is safe to evenly distribute the total thermal load from the building side to each DBHE. However, with the monitoring data from Xi'an and the data validated numerical model, we have shown in this

study that thermal interactions do exist and lead to about 12% shifted thermal load. This implies that, with different inter-borehole distances, amount of thermal load, and subsurface properties, the amount of performance reduction can also be different. Therefore, numerical models such as OpenGeoSys should be employed during the design procedure to predict the long-term sustainability of DBHE array. The drop in working fluid temperature should be simulated beforehand to make sure that it is maintained above a threshold value to make the system economically available.

### **CRedit authorship contribution statement**

**Wanlong Cai:** Conceptualization, Methodology, Software, Validation, Formal analysis, Writing - Original Draft, Visualization. **Fenghao Wang:** Conceptualization, Formal analysis, Project administration, Funding acquisition. **Shuang Chen:** Methodology, Software, Writing - Review & Editing, Visualization. **Chaofan Chen:** Methodology; Software, Investigation, Writing - Review & Editing. **Jun Liu:** Validation, Formal analysis, Investigation. **Jiewen Deng:** Validation, Data Curation. **Olaf Kolditz:** Project administration, Supervision. **Haibing Shao:** Methodology, Software, Writing - Review & Editing, Resources, Supervision.

### **Declaration of competing interest**

The authors declare that they have no known competing financial interests or personal relationships that could have appeared to influence the work reported in this paper.

### **Acknowledgements**

The research work is supported by Key Research and Development Project of Shaanxi Province (2020ZDLSF06-08), Open Project of Key Laboratory of Coal Resources Exploration and Comprehensive Utilization in Ministry of Natural Resources (KF2020-7). In addition, the first author (Wanlong Cai) would like to acknowledge the China Scholarship Council (CSC) for financially supporting his visiting PhD study in Germany.

## References

- [1] N. Zhao, F. You, Can renewable generation, energy storage and energy efficient technologies enable carbon neutral energy transition?, *Applied Energy* 279 (2020) 115889.
- [2] U. Lucia, M. Simonetti, G. Chiesa, G. Grisolia, Ground-source pump system for heating and cooling: Review and thermodynamic approach, *Renewable and Sustainable Energy Reviews* 70 (2017) 867–874.
- [3] J. M. Dias, V. A. Costa, Adsorption heat pumps for heating applications: A review of current state, literature gaps and development challenges, *Renewable and Sustainable Energy Reviews* 98 (2018) 317–327.
- [4] J. Lin, B. Lin, The actual heating energy conservation in china: Evidence and policy implications, *Energy and Buildings* 190 (2019) 195–201.
- [5] A. Anderson, B. Rezaie, Geothermal technology: Trends and potential role in a sustainable future, *Applied Energy* 248 (2019) 18–34.
- [6] Z. Pang, Y. Kong, H. Shao, O. Kolditz, Progress and perspectives of geothermal energy studies in china: from shallow to deep systems, *Geothermal Energy* (2018) 580.
- [7] L. Rybach, R. Hopkirk, Shallow and deep borehole heat exchangers—achievements and prospects, in: *Pro. World Geothermal Congress*, volume 1995, 1995, pp. 2133–2139.
- [8] T. Kohl, R. Brenni, W. Eugster, System performance of a deep borehole heat exchanger, *Geothermics* 31 (2002) 687–708.
- [9] A. Sapinska-Sliwa, M. A. Rosen, A. Gonet, T. Sliwa, Deep borehole heat exchangers—a conceptual and comparative review, *International Journal of Air-Conditioning and Refrigeration* 24 (2016) 1630001.
- [10] J. Deng, Q. Wei, M. Liang, S. He, H. Zhang, Field test on energy performance of medium-depth geothermal heat pump systems (md-ghps), *Energy and Buildings* 184 (2019) 289–299.
- [11] J. Liu, F. Wang, Y. Gao, Y. Zhang, W. Cai, M. Wang, et al, Influencing factors analysis and operation optimization for the long-term performance of medium-deep borehole heat exchanger coupled ground source heat pump system, *Energy and Buildings* (2020) 110385.

- [12] X. Song, G. Wang, Y. Shi, R. Li, Z. Xu, R. Zheng, et al, Numerical analysis of heat extraction performance of a deep coaxial borehole heat exchanger geothermal system, *Energy* 164 (2018) 1298–1310.
- [13] W. Cai, F. Wang, J. Liu, Z. Wang, Z. Ma, Experimental and numerical investigation of heat transfer performance and sustainability of deep borehole heat exchangers coupled with ground source heat pump systems, *Applied Thermal Engineering* 149 (2019) 975–986.
- [14] Y. Luo, H. Guo, F. Meggers, L. Zhang, Deep coaxial borehole heat exchanger: Analytical modeling and thermal analysis, *Energy* 185 (2019) 1298–1313.
- [15] R. A. Beier, Thermal response tests on deep borehole heat exchangers with geothermal gradient, *Applied Thermal Engineering* (2020) 115447.
- [16] L. Fang, N. Diao, Z. Shao, K. Zhu, Z. Fang, A computationally efficient numerical model for heat transfer simulation of deep borehole heat exchangers, *Energy and Buildings* 167 (2018) 79–88.
- [17] J. Liu, F. Wang, W. Cai, Z. Wang, Q. Wei, J. Deng, Numerical study on the effects of design parameters on the heat transfer performance of coaxial deep borehole heat exchanger, *International Journal of Energy Research* 43 (2019) 6337–6352.
- [18] X. Hu, J. Banks, L. Wu, W. V. Liu, Numerical modeling of a coaxial borehole heat exchanger to exploit geothermal energy from abandoned petroleum wells in hinton, alberta, *Renewable Energy* 148 (2020) 1110–1123.
- [19] T. Renaud, P. Verdin, G. Falcone, Numerical simulation of a deep borehole heat exchanger in the krafla geothermal system, *International Journal of Heat and Mass Transfer* 143 (2019) 118496.
- [20] M. Le Lous, F. Larroque, A. Dupuy, A. Moignard, Thermal performance of a deep borehole heat exchanger: Insights from a synthetic coupled heat and flow model, *Geothermics* 57 (2015) 157–172.
- [21] C. Chen, H. Shao, D. Naumov, Y. Kong, K. Tu, O. Kolditz, Numerical investigation on the performance, sustainability, and efficiency of the deep borehole heat exchanger system for building heating, *Geothermal Energy* 7 (2019) 18.

- [22] Z. Wang, F. Wang, J. Liu, Z. Ma, E. Han, M. Song, Field test and numerical investigation on the heat transfer characteristics and optimal design of the heat exchangers of a deep borehole ground source heat pump system, *Energy Conversion and Management* 153 (2017) 603–615.
- [23] J. Deng, S. He, Q. Wei, J. Li, H. Liu, Z. Zhang, et al, Field test and optimization of heat pumps and water distribution systems in medium-depth geothermal heat pump systems, *Energy and Buildings* 209 (2020) 109724.
- [24] X. Bu, Y. Ran, D. Zhang, Experimental and simulation studies of geothermal single well for building heating, *Renewable Energy* 143 (2019) 1902–1909.
- [25] Y. Huang, Y. Zhang, Y. Xie, Y. Zhang, X. Gao, J. Ma, Field test and numerical investigation on deep coaxial borehole heat exchanger based on distributed optical fiber temperature sensor, *Energy* (2020) 118643.
- [26] S. Koohi-Fayegh, M. A. Rosen, Examination of thermal interaction of multiple vertical ground heat exchangers, *Applied Energy* 97 (2012) 962–969.
- [27] P. Bayer, M. de Paly, M. Beck, Strategic optimization of borehole heat exchanger field for seasonal geothermal heating and cooling, *Applied energy* 136 (2014) 445–453.
- [28] A. Gultekin, M. Aydin, A. Sisman, Thermal performance analysis of multiple borehole heat exchangers, *Energy Conversion and Management* 122 (2016) 544–551.
- [29] O. Kolditz, S. Bauer, L. Bilke, N. Böttcher, J.-O. Delfs, T. Fischer, et al, Opegeosys: an open-source initiative for numerical simulation of thermo-hydro-mechanical/chemical (thm/c) processes in porous media, *Environmental Earth Sciences* 67 (2012) 589–599.
- [30] H.-J. G. Diersch, *FEFLOW: finite element modeling of flow, mass and heat transport in porous and fractured media*, Springer Science & Business Media, 2013.
- [31] H. Shao, P. Hein, A. Sachse, O. Kolditz, *Geoenergy Modeling II: Shallow Geothermal Systems*, Springer, 2016.

- [32] R. Al-Khoury, T. Kölbl, R. Schramedei, Efficient numerical modeling of borehole heat exchangers, *Computers & Geosciences* 36 (2010) 1301–1315.
- [33] H.-J. Diersch, D. Bauer, W. Heidemann, W. Rühaak, P. Schätzl, Finite element modeling of borehole heat exchanger systems: Part 1. fundamentals, *Computers & Geosciences* 37 (2011) 1122–1135.
- [34] H.-J. Diersch, D. Bauer, W. Heidemann, W. Rühaak, P. Schätzl, Finite element modeling of borehole heat exchanger systems: Part 2. numerical simulation, *Computers & Geosciences* 37 (2011) 1136–1147.
- [35] S. Chen, F. Witte, O. Kolditz, H. Shao, Shifted thermal extraction rates in large borehole heat exchanger array—a numerical experiment, *Applied Thermal Engineering* 167 (2020) 114750.
- [36] P. Hein, O. Kolditz, U.-J. Görke, A. Bucher, H. Shao, A numerical study on the sustainability and efficiency of borehole heat exchanger coupled ground source heat pump systems, *Applied Thermal Engineering* 100 (2016) 421–433.
- [37] L. Bilke, H. Shao, S. Chen, W. Cai, OpenGeoSys Tutorial, Website, 2020. <https://www.opengeosys.org/docs/userguide/basics/introduction/>.
- [38] F. Witte, I. Tuschy, TESPpy: Thermal Engineering Systems in Python, *Journal of Open Source Software* 5 (2020) 2178. doi:10.21105/joss.02178.
- [39] I. H. Bell, J. Wronski, S. Quoilin, V. Lemort, Pure and pseudo-pure fluid thermophysical property evaluation and the open-source thermophysical property library coolprop, *Industrial & engineering chemistry research* 53 (2014) 2498–2508.
- [40] D. Moldovan, F. Peeters, Pybinding v0.8.0: a Python package for tight-binding calculations, 2016. <https://doi.org/10.5281/zenodo.56818>.
- [41] F. Witte, TESPpy Documentation, <https://tespy.readthedocs.io/en/master>, 2020.
- [42] Y. Huang, Y. Zhang, Y. Xie, Y. Zhang, X. Gao, Thermal performance analysis on the composition attributes of deep coaxial borehole heat exchanger for building heating, *Energy and Buildings* 221 (2020) 110019.

- [43] N. Molina-Giraldo, P. Bayer, P. Blum, Evaluating the influence of thermal dispersion on temperature plumes from geothermal systems using analytical solutions, *International Journal of Thermal Sciences* 50 (2011) 1223–1231.
- [44] T. Xu, Z. Hu, B. Feng, G. Feng, F. Li, Z. Jiang, Numerical evaluation of building heating potential from a co-axial closed-loop geothermal system using wellbore–reservoir coupling numerical model, *Energy Exploration & Exploitation* 38 (2020) 733–754.
- [45] S. Chen, W. Cai, F. Witte, X. Wang, F. Wang, O. Kolditz, et al, Long-term thermal imbalance in large borehole heat exchangers array—a numerical study based on the leicester project, *Energy and Buildings* (2020) 110518.